First-principles study of the electronic structure and optical properties of defect chalcopyrite $CdGa_2Te_4$*

Jiao Zhao-Yong(焦照勇)†, Guo Yong-Liang(郭永亮),
Zhang Xian-Zhou(张现周)‡, and Ma Shu-Hong(马淑红)

College of Physics and Information Engineering, Henan Normal University, Xinxiang 453007, *China*

(Received 31 March 2012; revised manuscript received 14 May 2012)

The electronic and optical properties of the defect chalcopyrite $CdGa_2Te_4$ compound are studied based on the first-principles calculations. The band structure and density of states are calculated to discuss the electronic properties and orbital hybridized properties of the compound. The optical properties, including complex dielectric function, absorption coefficient, refractive index, reflectivity, and loss function, and the origin of spectral peaks are analysed based on the electronic structures. The presented results exhibit isotropic behaviours in a low and a high energy range and an anisotropic behaviour in an intermediate energy range.

Keywords: defect chalcopyrite $CdGa_2Te_4$, electronic structure, optical properties, first-principles calculation

PACS: 31.15.E–, 71.20.–b, 78.20.–e **DOI:** 10.1088/1674-1056/21/12/123101

1. Introduction

The ternary adamantine semiconductor compounds, $A^{II}B_2^{III}C_4^{IV}$ have been widely studied because of their promising applications to electro–optic, optoelectronic, and nonlinear optical devices.[1] Most of these compounds belong to the defect chalcopyrite type (space group: $I\bar{4}-S_4^2$, $Z=2$) as shown in Fig. 1, in which one of the cation sites is unoccupied. Among the defect chalcopyrite family, $CdGa_2Te_4$ and $CdGa_2Se_4$ have received much attention in recent years.[2–9] In the literature, a considerable anisotropy has been revealed in $CdGa_2Se_4$, based on the electronic dielectric function *ab initio* calculations. For the compound of $CdGa_2Te_4$, the bulk crystal was grown by the conventional Bridgman method.[10] Optical properties were studied[10–12] and the complex dielectric-function spectra were measured in a photon-energy range between 1.2 eV and 5.2 eV. The static dielectric constants of $CdGa_2Te_4$ were determined through infrared reflectivity spectra experiments.[13] The band structure was studied using first-principles calculation in Ref. [2], but neither the fine details of electronic structures nor optical properties have been studied for $CdGa_2Te_4$.

In the present paper, we aim at comprehensively studying the electronic structure and optical properties of $CdGa_2Te_4$, according to the density functional theory (DFT) calculations. Particularly, the partial density states of the $CdGa_2Te_4$ and the real and imaginary part of the electronic dielectric function, absorption coefficient, refractive index, reflectivity, and loss function are discussed and the present results are compared with the available related findings.

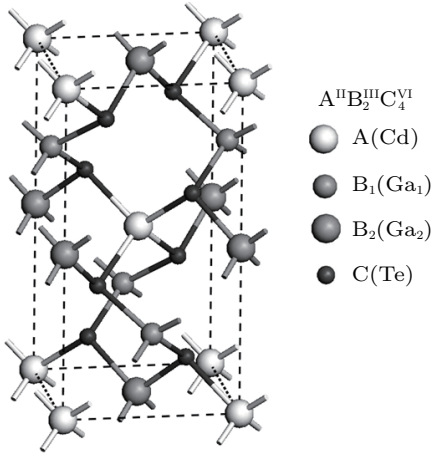


Fig. 1. Crystalline structure of defect chalcopyrite $A^{II}B_2^{III}C_4^{IV}$ ($CdGa_2Te_4$).

*Project supported by the Foundation for Key Program of Ministry of Education, China (Grant No. 212104) and the Foundation for University Young Core Instructors of Henan Province, China (Grant No. 2010GGJS-066).

†Corresponding author. E-mail: zhy_jiao@htu.cn

†E-mail: xz-zhang@htu.cn

© 2012 Chinese Physical Society and IOP Publishing Ltd

2. Computational details

All of the DFT calculations in this study are carried out using the Vienna *ab initio* simulation package (VASP)[13,14] with the ultrasoft potentials (USP) suggested by Vanderbilt[15] The exchange–correlation functional with generalized gradient approximation (GGA) of Perdew–Burke–Ernzerhof (PBE)[16] is used to solve the Kohn–Sham equations with a kinetic energy cutoff of 500 eV. The Brillouin-zone is sampled with a $8 \times 8 \times 4$ k-point mesh generated via the Monkhorst-pack scheme.[17] The geometry optimization is performed with ions, cell volume, and cell shape are allowed to change. The geometries are considered to be converged when the forces on each ion becomes 0.01 eV/Å (1 Å = 0.1 nm) or less. The convergence threshold is set to be 10^{-6} eV/atom for the total energy in the electronic self-consistent loop. The calculated structural parameters of the $CdGa_2Te_4$ compound are listed in Table 1, and the results are in good agreement with the available experimental results[18] within an error around 3% with respect to the experimental values.

Table 1. Calculated lattice constants, internal parameters, and bond lengths along with the available experimental values of $CdGa_2Te_4$.

	a/Å	c/Å	x	y	z	Cd-Te/Å	Ga_1–Te/Å	Ga_2–Te/Å
This work	6.278	12.00	0.272	0.255	0.137	2.887	2.686	2.664
Experiment[18]	6.1	11.7	0.27	0.26	0.135			

3. Results and discussion

3.1. Band structure and density of states

Based on the optimized structural results, electronic structures including the band structure, DOS, and PDOS are computed and shown in Figs. 2 and 3 for $CdGa_2Te_4$. The overall profile of the valence and conduction bands configuration of present results is in good agreement with previous calculations.[2] Our calculations give a direct band gap value of 1.047 eV, where the highest energy of valence bands and the lowest energy of conduction bands are both located at gamma point as shown in Fig. 2. This is in accordance with previous theoretical value of 1.08 eV[2] and less than the experimental result of 1.445 eV (T = 11 K).[11] In order to understand the bonding characteristics, figures 3(a)–3(d) show the total density of states (DOS) and partial density of states (PDOS) for $CdGa_2Te_4$. It can be seen from Fig. 3(a) that the valence band is divided into six parts labeled as A, B, C, D, E, and F. The lowest band (A) is located around −14.6 eV and it is dominated by the d-like states of Ga. The next band (B) ranging from −11.6 eV to −9.9 eV is divided into three narrow sub-bands in Fig. 3(a), owing to the contributions that come mainly from the Te and Ga s-like states. The third-lowest band (C) is centred at −8.0 eV and originates from the contributions of Cd d-like states. The sub-band D located in a range of about −6.3 eV to −4.6 eV is derived, and it comes mainly from the Ga s-like states and Te p-like states, and exhibits a double-peaked structure. The sub-band E ranging from −4.3 eV to −3.1 eV is contributed by Cd s-like states and Te p-like states. Finally, the top of the valence band (E)

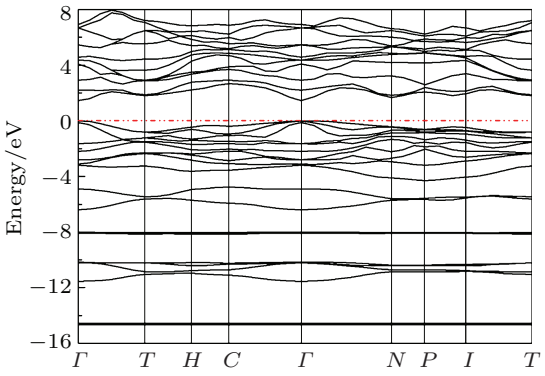


Fig. 2. Calculated band structure of the $CdGa_2Te_4$.

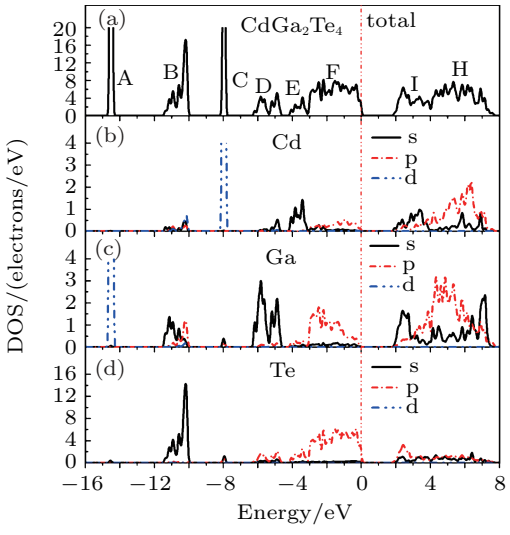


Fig. 3. Calculated total DOSs and PDOSs of $CdGa_2Te_4$.

is mainly composed of p-like states of Ga and Te. As shown in the PDOS of Figs. 3(b)–3(d), the p-like states of gallium and tellurium are highly hybridized around the top valence band of $CdGa_2Te_4$.

The conduction band can be divided into two regions: the lower energy region I (ranging from 1.8 eV to 4.0 eV) and the higher energy region II (ranging from 4.0 eV to 7.7 eV) (see Fig. 3(a)). The bottom of the conduction band (I) largely originates from the s-like states of Ga and p-like states of Te with a small mixing of Cd s-like states. The main contributions of the conduction band (II) come from p-like states of Ga and Cd, as well as the Ga s-like states at higher energies.

3.2. Optical properties

Consider the underestimated energy band gap of semiconductors within DFT–GGA approximations, optical properties calculated in the present paper for $CdGa_2Te_4$ are scissors corrected[19,20] by a value of 0.398 eV, which is the difference in energy gap between our calculated value (1.047 eV) and experimentally measured result (1.445 eV). The optical properties are obtained from the complex dielectric-function spectrum, $\varepsilon(\omega) = \varepsilon_1(\omega) + \mathrm{i}\varepsilon_2(\omega)$, which is related mainly to the electronic structure.[21] The imaginary part $\varepsilon_2(\omega)$ of the frequency-dependent dielectric function is calculated from the total DOS and the momentum matrix elements between the occupied and unoccupied eigenstates. The real part $\varepsilon_1(\omega)$ of the dielectric function can be extracted from $\varepsilon_2(\omega)$ using the Kramers–Kroning relationship. In our calculations, we neglect the contributions of intraband transition to $\varepsilon(\omega)$ due to its importance only for metal[22] and the insignificant contributions from the indirect interband transitions involving scattering of phonons. Only the direct interband transitions make an important contribution to $\varepsilon(\omega)$ and it is taken into consideration in the present calculation of the imaginary part of $\varepsilon(\omega)$. Calculated imaginary and real parts of $\varepsilon(\omega)$ are given in Fig. 4 and are compared with the experimental results[10] measured by spectroscopic ellipsometry (solid circles).

Figure 4(a) displays the variations of the imaginary part $\varepsilon_2(\omega)$ of the electronic dielectric function spectrum for a radiation up to 20 eV. We can see that the threshold energy of $\varepsilon_2(\omega)$ occurs at 1.45 eV. This is dominated by the direct optical transition from the highest valence band to the lowest conduction band at the gamma point, and it is known as the fundamental absorption edge. Beyond this energy, the $\varepsilon_2^{\perp}(\omega)$ (polarized along the direction perpendicular to the c-axis direction) and $\varepsilon_2^{\parallel}(\omega)$ (polarized along the direction parallel to the c-axis direction) curves increase rapidly. It is clear in Fig. 4(a) that the main peaks of $\varepsilon_2^{\perp}(\omega)$ and $\varepsilon_2^{\parallel}(\omega)$ are located at about 4.0 eV and 3.7 eV, respectively. Below the main peaks, there are two peaks located around 2.6 eV both for $\varepsilon_2^{\perp}(\omega)$ and $\varepsilon_2^{\parallel}(\omega)$, and a similar case is viewed above the main peak at about 4.8 eV for $\varepsilon_2^{\perp}(\omega)$ and 4.5 eV for $\varepsilon_2^{\parallel}(\omega)$, respectively. Accordingly, the experimental measurements[10] show the peaks at 3.8 eV (main peak), 3.1 eV, and 5.0 eV as seen in Fig. 4(a) (black dotted lines). Moreover, it is noted that in the lower and higher energy range both $\varepsilon_2^{\perp}(\omega)$ and $\varepsilon_2^{\parallel}(\omega)$ exhibit isotropic behaviours, while in the inter-mediate energies an anisotropic behaviour is shown. Additionally, calculated static dielectric constants of $\varepsilon_1^{\perp}(0)$ and $\varepsilon_1^{\parallel}(0)$, corresponding to the low energy limit of $\varepsilon_1(\omega)$ in Fig. 4(b), are listed in Table 2,

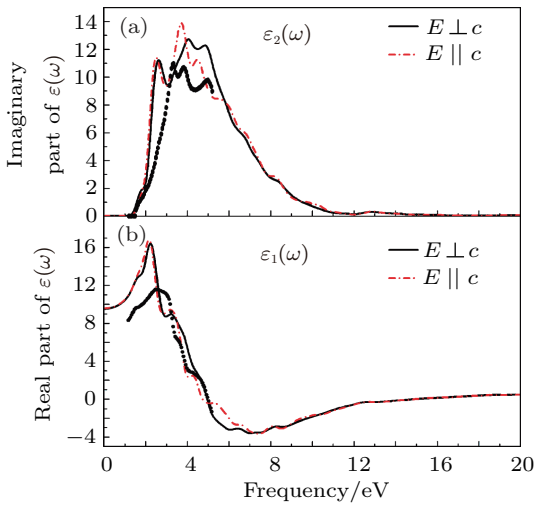


Fig. 4. Calculated imaginary and real parts of the frequency-dependent dielectric function $\varepsilon(\omega)$ of $CdGa_2Te_4$. The solid circles represent experimental results reported by Ozaki *et al.*[10]

Table 2. Calculated and experimental values of static constants $\varepsilon_1^{\perp}(0)$, $\varepsilon_1^{\parallel}(0)$, $n^{\perp}(0)$, and $n^{\parallel}(0)$.

	This work	Experiment[23]
$\varepsilon_1^{\perp}(0)$	9.53	12.04
$\varepsilon_1^{\parallel}(0)$	9.56	11.47
$n^{\perp}(0)$	3.09	
$n^{\parallel}(0)$	3.09	

which are slightly less than the experimental results reported by Nikolić and Stojilković.[23] And our calculated curves of $\varepsilon_1^{\perp}(0)$ and $\varepsilon_1^{\parallel}(0)$ are in accordance with the experimental curves[10] in Fig.4(b) (solid circles).

Calculated absorption coefficient $\alpha(\omega)$, refractive index $n(\omega)$, and $k(\omega)$, reflectivity spectrum $R(\omega)$ and loss function $L(\omega)$, derived from $\varepsilon_1(\omega)$ and $\varepsilon_2(\omega)$ are presented in Fig. 5 for $CdGa_2Te_4$. It can be seen from Fig. 5(a) that the absorption edge starts from the energy value of 1.445 eV, corresponding to the energy gap of $\Gamma_v - \Gamma_c$ for the compound. The refractive indexes including $n(\omega)$ and $k(\omega)$ as shown in Fig. 5(b) reach maximal values of about 4.20 and 4.26 at 2.27 eV and 2.23 eV for $n^{\perp}(\omega)$ and $n^{\parallel}(\omega)$, respectively, and indicate an anisotropy between the direction perpendicular and the direction parallel to the c-axis direction in the intermediate energies. Both for $n^{\perp}(\omega)$ and $n^{\parallel}(\omega)$, the refractive indexes both reach a maximal value of 4.22 around 2.27 eV, and $n^{\perp}(0)$ and $n^{\parallel}(0)$ are predicted to have the same value of 3.09 as listed in Table 2. In Fig. 5(c), computed reflectivity spectra $R^{\perp}(\omega)$ and $R^{\parallel}(\omega)$ also show an anisotropic behaviour each. The loss function $L(\omega)$ plotted in Fig. 5(d) displays a shoulder-like peak located at 12.6 eV, corresponding to the first abrupt reduction of the reflectivity spectrum $R(\omega)$. In Fig. 5(d), the main peak of the loss function located at 14.9 eV determines the screened plasma frequency ω_p[24] and corresponds to the second abrupt reduction of $R(\omega)$ and to the zero crossing of $\varepsilon_1(\omega)$.

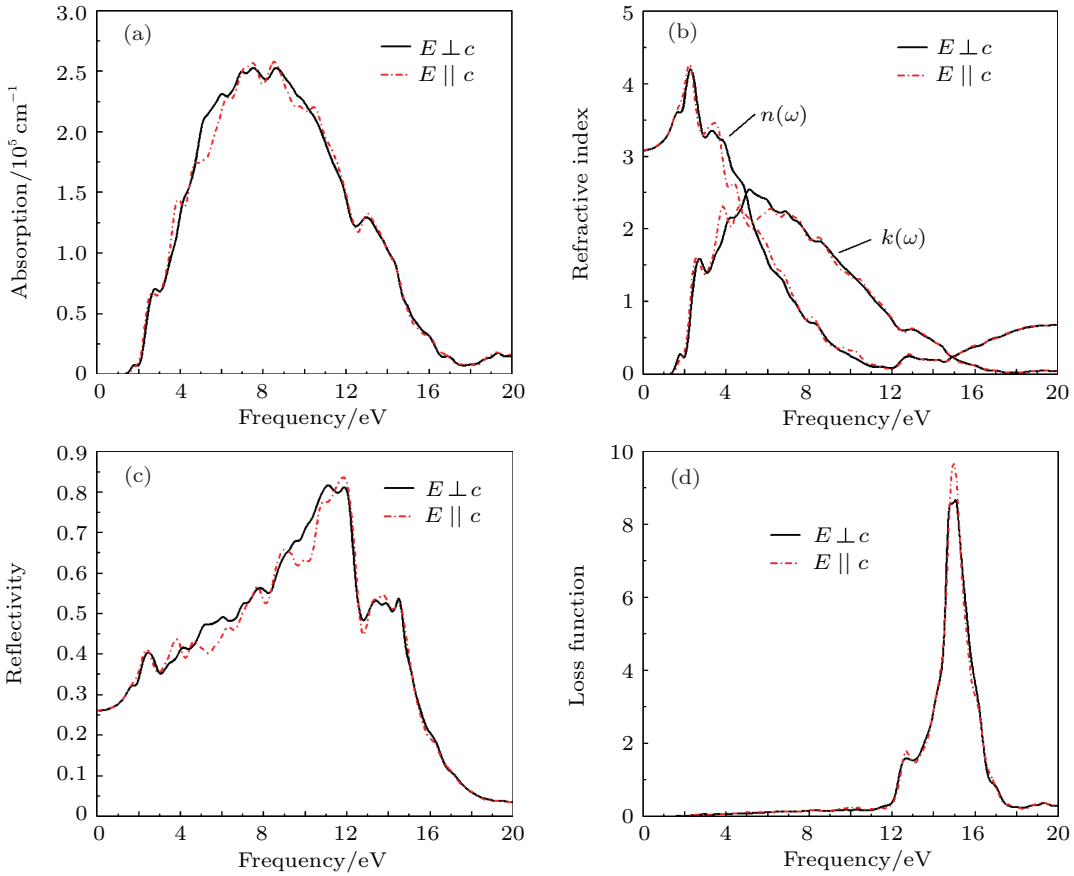


Fig. 5. Calculated values of optical absorption coefficient $\alpha(\omega)$, refractive indexes $n(\omega)$ and $k(\omega)$, reflectivity spectrum $R(\omega)$, and loss function $L(\omega)$ for $CdGa_2Te_4$.

4. Conclusions

In this paper, we studied the electronic and optical properties of $CdGa_2Te_4$ using the first-principles calculation. The results show that $CdGa_2Te_4$ is a direct band gap semiconductor with an underestimated gap value of 1.047 eV compared with the experimental value of 1.445 eV. The p-like states of Ga and Te are highly hybridized in the upper part of the valence band of $CdGa_2Te_4$, while the bottom of the conduction band largely originates from the s-like states of Ga and p-like states of Te with a small mixing of Cd

s-like states. The analysis of optical properties indicates that the defect chalcopyrite $CdGa_2Te_4$ exhibits an anisotropic behaviour in the intermediate energies, similar to the compound of $CdGa_2Se_4$.

References

[1] Georgobiani A N, Radautsan S I and Tiginyanu I M 1985 *Sov. Phys. Semicond.* **19** 121

[2] Jiang X S and Lambrecht W R L 2004 *Phys. Rev.* B **69** 035201

[3] Manjón F J, Gomis O, Rodríguez-Hernández P, Pérez-González E, Muñoz A, Errandonea D, Ruiz-Fuertes J, Segura A, Fuentes-Cabrera M, Tiginyanu I M and Ursaki V V 2010 *Phys. Rev.* B **104** 063524

[4] Errandonea D, Kumar R S, Manjón F J, Ursaki V V and Tiginyanu I M 2008 *J. Appl. Phys.* **104** 063524

[5] Lavrentyev A A, Gabrelian B V, Nikiforov I Ya, Parasyuk O V and Khyzhun O Yu 2009 *J. Alloys Compd.* **481** 28

[6] Grzechnik A, Ursaki V V, Syassen K, Loa I, Tiginyanu I M and Hanfland M 2001 *J. Solid State Chem.* **160** 205

[7] Jiang X S, Yan Y C, Yuan S M, Mi S, Niu Z G and Liang J Q 2010 *Chin. Phys.* B **19** 107104

[8] Ma S H, Jiao Z Y and Zhang X Z 2012 *J. Mater. Sci.* **47** 3849

[9] Jiang X S, Mi S, Sun P J, Lu Y and Liang J Q 2009 *Chin. Phys. Lett.* **26** 077102

[10] Ozaki S, Muto K and Adachi S 2003 *J. Phys. Chem. Solids* **64** 1935

[11] Ozaki S, Muto K, Nagata H and Adachi S 2005 *J. Appl. Phys.* **97** 043507

[12] Sasaki M, Ozaki S and Adachi S 2005 *Phys. Rev.* B **72** 045218

[13] Kresse G and Furthmüller J 1996 *Phys. Rev.* B **54** 11169

[14] Kresse G and Furthmüller J 1996 *Comput. Mater. Sci.* **6** 15

[15] Vanderbilt D 1990 *Phys. Rev.* B **41** 7892

[16] Perdew J P, Burke K and Ernzerhof M 1996 *Phys. Rev. Lett.* **77** 3865

[17] Monkhorst H J and Pack J D 1976 *Phys. Rev.* B **13** 5189

[18] Hahn H, Frank G, klingler W, Störger A D and Störger G 1955 *Anorg Z Allg. Chem.* **279** 241

[19] Godby R W, Schlüter M and Sham L J 1988 *Phys. Rev.* B **37** 10159

[20] Hybertsen M S and Louie S G 1986 *Phys. Rev.* B **34** 5390

[21] Li D and Zhang X H 2011 *Chin. Phys.* B **20** 126102

[22] Reshak A H, Atuchin V V, Auluck S and Kityk I V 2008 *J. Phys.*: *Condens. Matter* **20** 325234

[23] Nikolić P M and Stojilković S 1981 *J. Phys.* C **14** L551

[24] Fox M 2001 *Optical Properties of Solids* (New York: Oxford University Press) p. 12